Magnetohydrodynamic nanofluid flow and heat transfer along a permeable stretching surface with non uniform heat generation/absorption

Md. S. Ansari*, R. Nandkeolyar, S. S. Motsa

School of Mathematics, Statistics &Computer Science, University of KwaZulu-Natal, Pietermaritzburg-3209, South Africa

Abstract

This paper investigates the flow of a nano fluid past a stretching permeable sheet under the influence of transverse magnetic field. The space and temperature dependent heat source/sink effect is considered. The governing partial differential equations are transformed into ordinary differential equations with the help suitable similarity transformation. The transformed ordinary differential equations are solved using Spectral Relaxation Method. To validate the accuracy of the method, a comparison of Nusselt and Sherwood number with the data of previous work is presented,which shows an excellent agreement. The effects of magnetic field, suction, space and temperature dependent heat sourcr/sink, Lewis number, thermophoresis and Brownian motion on the flow field, temperature and nanofluid particle concentration are studied with the help of graphs and tables.

Keywords: Magnetic field, Nanofluid, Non uniform heat source/sink, Spectral Relaxation Method, similar solution

1. Introduction

Nanofluids are suspensions of nanoparticles (nominally 1-100nm in size) in conventional base fluids such as water, oils or glycols. The nanoparticles used in nanofluids are typically made of metals, carbides, oxides or carbon nanotubes. Nanofluids have interesting properties that make them potentially useful in many applications in heat transfer [1] including microelectronics, fuel cells, pharmaceutical processes, and hybrid-powered engines, engine cooling/vehicle thermal management, domestic refrigerator, chiller, heat exchanger, nuclear reactor coolant, in grinding, in space technology, defense and ships, and in boiler flue gas temperature reduction. They exhibit enhanced thermal conductivity and the convective heat transfer coefficient compared to the base fluid [2]. Choi [3] is the first who used the term nanofluids to refer to the fluid with suspended nano particles. Choi et al [4] reported that addition of small amount (less than 1% by volume) of nanoparticles to conventional heat transfer liquids increased the thermal conductivity of the fluid upto approximately two times.

Magnetohydrodynamic boundary layer flow of nanofluid and heat transfer over a linear stretching sheet has diverse applications in industrial, scientific and engineering problems such as boundary layer flow control, MHD power generators, micro MHD pumps, the cooling of nuclear reactors, plasma studies, geothermal energy extraction, cooling of large metallic plates in bathes, micro mixing of physiological samples, biological transportation and drug delivery [5, 6, 7]. Crane [8] was the first to analyze boundary layer flow of a Newtonian fluid induced by a stretching of elastic sheet moving in its own plane linearly. Several researchers [9, 10, 11, 12, 13] studied analytically/numerically the various aspects of problem of nanofluid flow over a stretching surface under different conditions. Salari et al. [14] analyzed numerically the heat transfer of nanofluid over a flat stretching sheet considering two sets of boundary conditions viz (i) a constant and (ii) a linear streamwise variation of nanoparticle volume fraction and wall temperature. The boundary layer flow and heat transfer over a permeable stretching sheet due to a nanofluid under the influence of external magnetic field, slip boundary condition and thermal radiation was investigated by Ibrahim and Shankar [15]. Ibrahim et al. [16] studied theoretically the effect of magnetic field on stagnation point flow and heat transfer of nanofluid flow over a stretching sheet. It was reported that the heat transfer rate at the surface increases with the magnetic parameter when the free stream velocity exceeds the stretching sheet velocity. Makinde

*Corresponding author

Email addresses: shariffuddin@gmail.com (Md. S. Ansari), rajnandkeolyar@gmail.com (R. Nandkeolyar), sandilemotsa@gmail.com (S. S. Motsa)

et al. [17] analyzed the combined effects of buoyancy force, convective heating, Brownian motion and thermophoresis on the stagnation point flow and heat transfer of an electrically conducting nanofluid towards a stretching sheet under the influence of magnetic field. Qasim et al. [18] investigated the problem of magnetohydrodynamic flow of ferrofluid along a stretching cylinder with velocity slip and prescribed surface heat flux. Bhattacharyya and Layek [19] considered the boundary layer flow of a nanofluid due to an exponentially permeable stretching sheet with external magnetic field.

The study of temperature dependent heat source/sink on the heat transfer characteristics is interesting owing to significant temperature differences between the surface and ambient-fluid in various engineering applications. The effect of space- and temperature dependent internal heat generation/absorption on the heat transfer characteristics of the flow have been studied by several researchers [20, 21, 22, 23, 24, 25] under different conditions and configurations. Abel and Mahantesh [26] presented an analytical solution of the viscoelastic fluid flow and heat transfer over a stretching sheet under the influence of non uniform heat source/sink and uniform magnetic field. Ramesh et al. [27] investigated numerically the steady MHD flow of a dusty fluid near the stagnation point past a permeable stretching sheet with the effect of non-uniform heat source/sink. In view of the above referred works we consider the flow of nano fluid past a permeable stretching sheet under the influence of an external magnetic field taking into account the effect of the space and temperature dependent heat source/sink. The nonlinear governing partial differential equations for the flow, energy and nanoparticle concentration are transformed into ordinary differential equations using similarity transformation and are then solved numerically by Spectral Relaxation Method.

2. Mathematical Formulation

Consider two dimensional steady boundary layer flow of a viscous, incompressible, electrically conducting, heat generating/ absorbing nanofluid past a stretching sheet in a quiescent fluid. The velocity of stretching sheet is $U_w = ax$ (where $a > 0$ is the constant acceleration parameter). The x axis is taken along the sheet in vertically upward direction and y axis is taken normal to the sheet. The surface of the sheet is maintained at uniform temperature and concentration, T_w and C_w, respectively, and these values are assumed to be greater than the ambient temperature and concentration, T_∞ and C_∞, respectively. The whole system is permeated by a uniform transverse magnetic field B_0 which is applied parallel to y axis. The induced magnetic field is neglected in comparison to applied one. It is assumed that both the fluid and nanoparticles are in thermal equilibrium state. The thermo physical properties of the nanofluid are assumed to be constant. The pressure gradient and external forces are neglected. In addition, the fluid suction is imposed at the sheet surface in the y direction.

Under the above assumptions and usual boundary layer approximation, the magnetohydrodynamic steady nanofluid flow, heat and mass transfer with internal heat generation/absorption are governed by the following equations:

The continuity equation

$$\frac{\partial u}{\partial x} + \frac{\partial v}{\partial y} = 0 \tag{1}$$

The momentum equation

$$u\frac{\partial u}{\partial x} + v\frac{\partial u}{\partial y} = \nu\frac{\partial^2 u}{\partial y^2} - \frac{\sigma B_0^2}{\rho_f}u \tag{2}$$

The energy equation

$$u\frac{\partial T}{\partial x} + v\frac{\partial T}{\partial y} = \alpha\frac{\partial^2 T}{\partial y^2} + \tau\left[D_B\frac{\partial C}{\partial y}\frac{\partial T}{\partial y} + \frac{D_T}{T_\infty}\left(\frac{\partial T}{\partial y}\right)^2\right] + \frac{q'''}{(\rho c)_f} \tag{3}$$

The nanoparticle concentration equation

$$u\frac{\partial C}{\partial x} + v\frac{\partial C}{\partial y} = D_B\frac{\partial^2 C}{\partial y^2} + \frac{D_T}{T_\infty}\frac{\partial^2 T}{\partial y^2} \tag{4}$$

where u and v are velocity components along x and y directions, respectively. $\alpha, \nu, \rho, c, (\rho c)_p, (\rho c)_f, D_B, D_T$ and τ are, respectively, thermal diffusivity, kinematic viscosity, mass density, specific heat, effective heat capacity of the nanoparticle material, heat capacity of the fluid, Brownian diffusion coefficient, thermophoresis diffusion coefficient and a parameter defined by $(\rho c)_p / (\rho c)_f$.

The associated boundary conditions are

$$\text{At } y = 0: \ u = U_w(x) = ax, \ v = -V_0; \ T = T_w; \ C = C_w \tag{5}$$

$$\text{As } y \to \infty: \ u \to 0; \ T \to T_\infty; \ C \to C_\infty \tag{6}$$

In order for similarity condition to exist, the nonuniform heat source/sink q''' is modeled as [28]

$$q''' = \left(\frac{kU_w(x)}{x\nu}\right)\left[A^*(T_w - T_\infty) f' + B^*(T - T_\infty)\right] \tag{7}$$

where k is thermal conductivity, A^* and B^* are parameters of space-dependent and temperature-dependent heat generation/absorption. Both A^* and B^* positive corresponds to internal heat source and negative to internal heat sink.

To transform the governing equations into a set of similarity equations, the following transformations are introduced

$$\eta = \sqrt{\frac{a}{\nu}}y, \ \psi(x,y) = \sqrt{a\nu}xf(\eta), \ \theta = \frac{T - T_\infty}{T_w - T_\infty}, \ \phi = \frac{C - C_\infty}{C_w - C_\infty} \tag{8}$$

where ψ is the stream function, $f(\eta)$ is a dimensionless stream function, θ is dimensionless temperature, ϕ is dimensionless concentration function and η is similarity variable. Continuity equation is satisfied if the velocity components are taken as

$$u = \frac{\partial \psi}{\partial y}, \quad v = -\frac{\partial \psi}{\partial x} \tag{9}$$

Eqns. (1)-(4), after similarity transfomation, are

$$f''' + ff'' - f'^2 - Mf' = 0 \tag{10}$$

$$\frac{1}{P_r}\left\{\theta'' + (A^* f' + B^* \theta)\right\} + f\theta' + N_b\phi'\theta' + N_t\theta'^2 = 0 \tag{11}$$

$$\phi'' + Lef\phi' + \frac{N_t}{N_b}\theta'' = 0 \tag{12}$$

and the associated boundary conditions become

$$f'(0) = 1, \ f(0) = S, \ \theta(0) = 1, \ \phi(0) = 1, \qquad f'(\infty) \to 0, \ \theta(\infty) \to 0, \ \phi(\infty) \to 0 \tag{13}$$

where

$$\left.\begin{aligned} M &= \frac{\sigma B_0^2}{a\rho}, \\ P_r &= \frac{\nu}{\alpha}, \\ N_b &= \frac{\tau D_B (C_w - C_\infty)}{\nu}, \\ N_t &= \frac{\tau D_T (T_w - T_\infty)}{\nu T_\infty}, \\ Le &= \frac{\nu}{D_B}, \\ S &= \frac{V_0}{\sqrt{a\nu}} \end{aligned}\right\} \text{governing parameters}$$

where M, P_r, N_b, N_t, Le and S are, respectively, magnetic parameter, Prandtl number, Brownian motion parameter, thermophoresis parameter, Lewis number and suction parameter.

The physical quantities of interest, the local skin friction coefficient Cf_x, the local Nusselt number Nu_x and the local Sherwood number Sh_x, are defined as:

$$Cf_x Re_x^{1/2} = f''(0), \tag{14}$$

$$Nu_x Re_x^{-1/2} = -\theta'(0), \tag{15}$$

$$Sh_x Re_x^{-1/2} = -\phi'(0). \tag{16}$$

where $Re_x = \frac{U_w x}{\nu}$ is the local Reynolds number.

3. Solution Technique

To solve the non linear boundary value problem described by eqns. (10)-(13), we adopted the spectral relaxation method (SRM) [29]. To apply SRM on eqns. (10)-(13), we set $f'(\eta) = g(\eta)$ then the eqns. (10)-(12) reduce to the following system of equations :

$$f' = g, \tag{17}$$
$$g'' + fg' - g^2 - Mg = 0, \tag{18}$$
$$\frac{1}{P_r}\{\theta'' + (A^* f' + B^* \theta)\} + f\theta' + N_b \phi'\theta' + N_t \theta'^2 = 0, \tag{19}$$
$$\phi'' + Lef\phi' + \frac{N_t}{N_b}\theta'' = 0, \tag{20}$$

and the boundary conditions (13) become

$$g(0) = 1,\ f(0) = S,\ \theta(0) = 1,\ \phi(0) = 1, \qquad g(\infty) \to 0,\ \theta(\infty) \to 0,\ \phi(\infty) \to 0 \tag{21}$$

In framework of SRM, writing the iteration scheme as

$$f'_{r+1} = g_r, \quad f_{r+1}(0) = S, \tag{22}$$
$$g''_{r+1} + f_{r+1}g'_{r+1} - Mg_{r+1} = g_r^2, \quad g_{r+1}(0) = 1, \quad g_{r+1}(\infty) = 0, \tag{23}$$
$$\theta''_{r+1} + P_r f_{r+1}\theta'_{r+1} + B^*\theta_{r+1} = -\left(P_r N_b \phi'_r \theta'_r + P_r N_t \theta'^2_r + A^* g_{r+1}\right),\ \theta_{r+1}(0) = 1,\ \theta_{r+1}(\infty) = 0, \tag{24}$$
$$\phi''_{r+1} + Lef_{r+1}\phi'_{r+1} = -\frac{N_t}{N_b}\theta''_{r+1},\ \phi_{r+1}(0) = 1,\ \phi_{r+1}(\infty) = 0, \tag{25}$$

The domain is $0 \le \eta \le \eta_\infty$ and η_∞ is the edge of the boundary layer. Using the mapping $\xi = \frac{2\eta}{\eta_\infty} - 1$ the domain $[0, \eta_\infty]$ is mapped into the computational domain $[-1, 1]$. Defining the grid points $\xi_j = cos\left(\frac{\pi j}{N}\right)$, where N is the number of grid points, $j = 0, 1, 2, ..., N$. Applying the Chebyshev pseudo-spectral method on eqns. (22)-(25), we obtain

$$A_1 \mathbf{f_{r+1}} = \mathbf{B_1},\ \mathbf{f_{r+1}}(\xi_\mathbf{N}) = \mathbf{S}, \tag{26}$$
$$A_2 \mathbf{g_{r+1}} = \mathbf{B_2},\ \mathbf{g_{r+1}}(\xi_\mathbf{N}) = \mathbf{1},\ \mathbf{g_{r+1}}(\xi_\mathbf{0}) = \mathbf{0} \tag{27}$$
$$A_3 \theta_{r+1} = B_3, \quad \theta_{r+1}(\xi_N) = 1,\ \theta_{r+1}(\xi_0) = 0 \tag{28}$$
$$A_4 \phi_{r+1} = B_4, \quad \phi_{r+1}(\xi_N) = 1,\ \phi_{r+1}(\xi_0) = 0, \tag{29}$$

where

$$A_1 = \mathbf{D},\ \mathbf{B_1} = \mathbf{g_r}$$
$$A_2 = \mathbf{D^2} + \mathbf{diag}\left[\mathbf{f_{r+1}}\right]\mathbf{D} - \mathbf{MI},\ \mathbf{B_2} = \mathbf{g_r^2} \tag{30}$$
$$A_3 = \mathbf{D^2} + \mathbf{diag}\left[\mathbf{P_r f_{r+1}}\right]\mathbf{D} + \mathbf{B^* I},\ \mathbf{B_3} = -\left[\mathbf{P_r N_b}\phi'_\mathbf{r}\theta'_\mathbf{r} + \mathbf{P_r N_t}\theta'^\mathbf{2}_\mathbf{r} + \mathbf{A^* g_{r+1}}\right] \tag{31}$$
$$A_4 = \mathbf{D^2} + \mathbf{diag}\left[\mathbf{Lef_{r+1}}\right]\mathbf{D},\ \mathbf{B_4} = -\frac{\mathbf{N_t}}{\mathbf{N_b}}\theta''_\mathbf{r+1} \tag{32}$$

with $\mathbf{I}$ and $\mathbf{D}$ are being an identity and differentiation matrix, respectively. $\mathbf{f}, \mathbf{g}, \theta$ and ϕ are the values of functions f, g, θ and ϕ,respectively, computed at the grid points. The initial approximations satisfying the boundary conditions, used to start the iteration process, are $f_0(\eta) = S - e^{-\eta} + 1, g_0(\eta) = e^{-\eta}, \theta_0(\eta) = e^{-\eta}$ and $\phi_0(\eta) = e^{-\eta}$.

4. Results and Discussion

To demonstrate the accuracy of our numerical results, Table 1 and 2 are the values of $-\theta'(0)$ and $-\phi'(0)$ for the case when $M = 0, A^* = 0, B^* = 0$ and $S = 0$ between our calculations and the data presented by Khan and Pop[9]. These tables show that the agreement is very good. Fig. 1 shows the distribution of dimentionless velocity $f'(\eta)$, temperature $\theta(\eta)$ and nanoparticle volume fraction $\phi(\eta)$ for different values of magnetic parameter M. The velocity

Table 1: Comparison of the results for reduced Nusselt number $-\theta'(0)$

N_b	N_t	Present results $M = A^* = B^* = S = 0$	Khan and Pop[9]
0.1	0.1	0.9524	0.9524
	0.2	0.6932	0.6932
	0.3	0.5201	0.5201
0.2	0.1	0.5056	0.5056
	0.2	0.3654	0.3654
	0.3	0.2731	0.2731
0.3	0.1	0.2522	0.2522
	0.2	0.1816	0.1816
	0.3	0.1355	0.1355

Table 2: Comparison of the results for reduced Sherwood number $-\phi'(0)$

N_b	N_t	Present results $M = A^* = B^* = S = 0$	Khan and Pop [9]
0.1	0.1	2.1294	2.1294
	0.2	2.2740	2.2740
	0.3	2.5286	2.5286
0.2	0.1	2.3819	2.3819
	0.2	2.5152	2.5152
	0.3	2.6555	2.6555
0.3	0.1	2.4100	2.4100
	0.2	2.5150	2.5150
	0.3	2.6088	2.6088

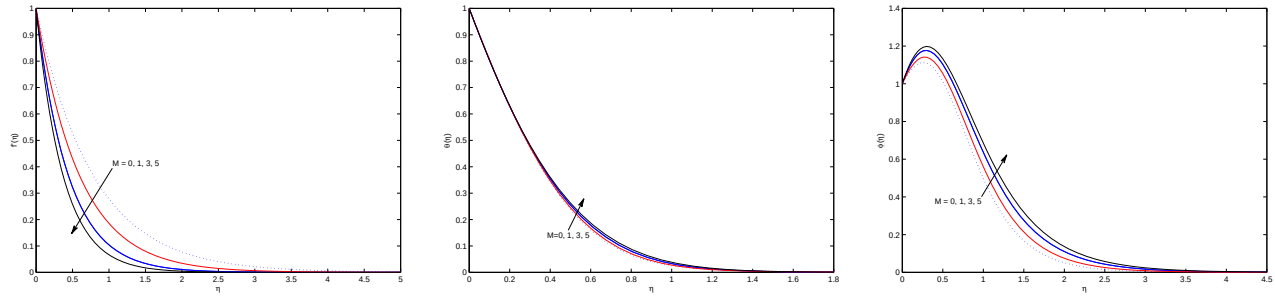

(a) (b) (c)

Figure 1: Effect of magnetic parameter M on (a) f', (b) θ, and (c) ϕ when $Pr = 6.7850,\ N_t = 0.3,\ N_b = 0.2,\ Le = 2,\ A^* = 0.2,\ B^* = 0.2,$ and $S = 0.5$

reduces with the increase in Magnetic parameter. The presence of magnetic field in an electrically conducting fluid tends to produce a body force against the flow. This type of resistive force tends to slow down the motion of the fluid in the boundary layer which, in turn, increases the temperature and nanoparticle volume fraction, this is exactly what we observe in Fig. 1. Consequently, the thermal boundary layer thickness and nanoparticle volume fraction boundary layer thickness become thicker for stronger magnetic field. The nanoparticle volume fraction $\phi(\eta)$ is higher in the fluid near to the sheet than the value at the wall. Since the fluid flow is caused solely by the stretching sheet and the sheet surface temperature and concentration is higher than free stream temperature and concentration, the velocity, temperature and nano particle concentration decrease with increasing η. Fig 2 depicts the influence of

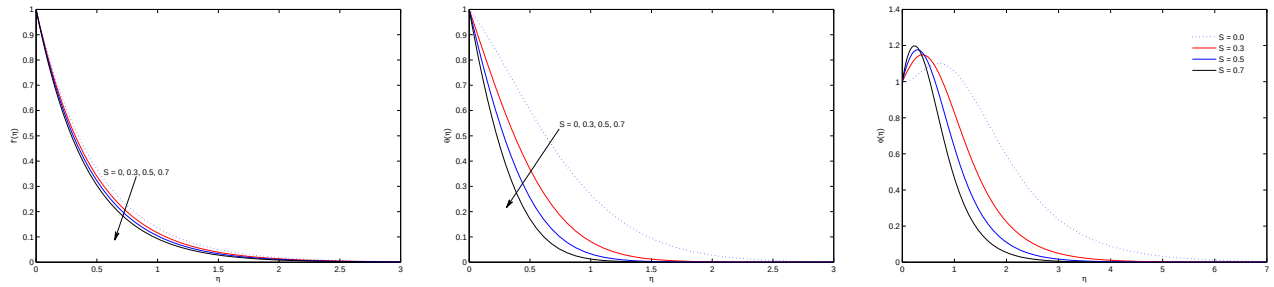

(a) (b) (c)

Figure 2: Effect of suction parameter S on (a) f', (b) θ, and (c) ϕ when $Pr = 6.7850,\ N_t = 0.3,\ N_b = 0.2,\ Le = 2,\ A^* = 0.2,\ B^* = 0.2$, and $M = 3$

suction parameter S on the velocity, temperature and nanoparticle volume fraction profiles in the boundary layer respectively. Due to imposition of wall suction, the fluid is brought closer to the sheet and it reduces momentum boundary layer thickness as well as the thermal and nanoparticle volume boundary layer thicknesses. This causes reduction in the velocity, temperature and particle volume fraction profiles. These effects are obvious from Fig 2. The nanoparticle volume fraction exhibits overshoot near the stretching sheet. The temperature and particle

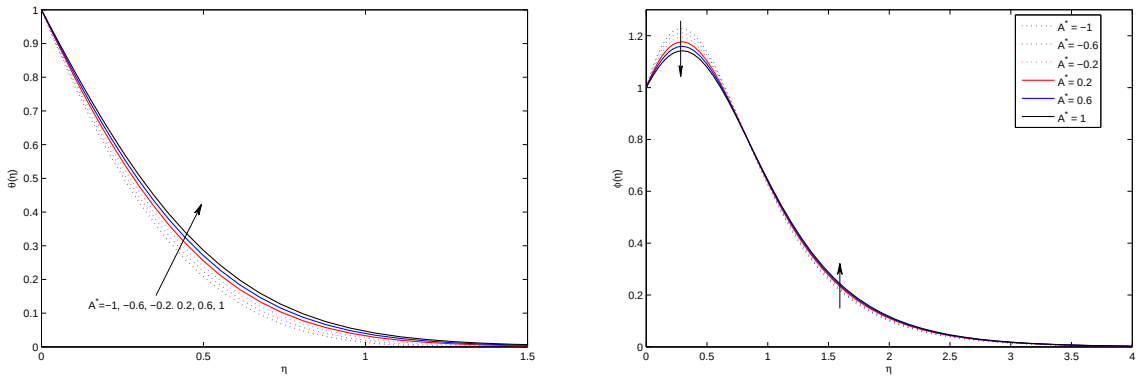

(a) (b)

Figure 3: Effect of space-dependent parameter for heat source/sink A^* on (a) θ, and (b) ϕ with $Pr = 6.7850,\ N_t = 0.3,\ N_b = 0.2,\ Le = 2,\ S = 0.5,\ B^* = 0.2$, and $M = 3$

volume fraction profiles for different space-dependent and temperature-dependent parameters for heat source/sink are presented in Figs. 3 and 4. On increasing values of A^* and/ or B^* produce increase in the temperature distributions of the nanofluid. This is expected since the presence of heat source $A^* > 0$ and/ or $B^* > 0$ in the boundary layer generates energy which causes the temperature of the fluid to increase. Heat sink ($A^* < 0$) and/ or $B^* < 0$ has the opposite effect, namely cooling of the fluid. The profiles show that the effects of A^* and B^* on the distribution of solid volume fraction of nanofluid on the boundary layer region. Near the plate, the volume fraction of nanofluid decrease as the heat source $A^* > 0$ and/ or $B^* > 0$ increase but the effect is opposite in the region away from the

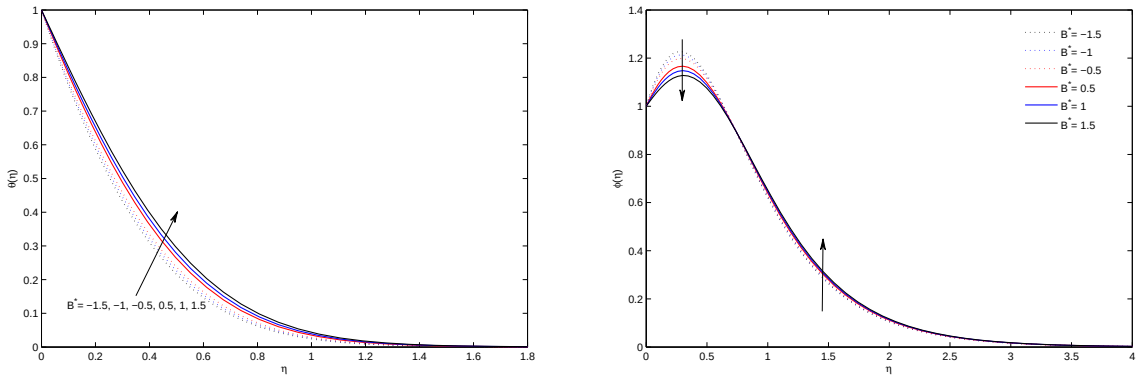

(a) (b)

Figure 4: Effect of temperature-dependent parameter for heat source/sink B^* on (a) θ, and (b) ϕ with $Pr = 6.7850,\ N_t = 0.3,\ N_b = 0.2,\ Le = 2,\ S = 0.5,\ A^* = 0.2$, and $M = 3$

plate (closer to the free stream). On the contrary, a reverse effect is observed on particle volume fraction due to the heat sink ($A^* < 0$) and/ or $B^* < 0$. The volume fraction curves exhibit peaks with concentrations in the boundary layer exceeding the concentration at the wall. The thermal field exerts forces on all molecules and nano particles in the nanofluid forcing them to move, in the direction of the heat flow, i.e., from the hot side to the cold side. The

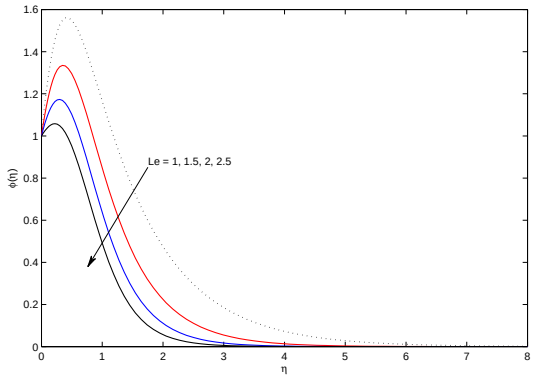

(a)

Figure 5: Effects of Le on concentration profiles with $Pr = 6.7850,\ N_t = 0.3,\ N_b = 0.2,\ S = 0.5,\ \ A^* = 0.2,\ B^* = 0.3$, and $M = 3$

variation of nanoparticle concentration for various values of Lewis number is shown in Fig 5. It is observed that Lewis number significantly affects the concentration distribution. There is decrease in volume fraction on increasing Lewis number, since higher Lewis number implies a lower Brownian diffusion coefficient D_B which result in a shorter penetration depth for the concentration boundary layer. It is also noticed that the volume fraction initially increases near the sheet and after attaining a peak it decreases away from the sheet for smaller values of Le. Fig. 6 presents the effects of the Bownian motion and thermophoresis effect on the temperature distribution. The figure reveals that the temperature of the fluid increases with increasing values of N_t and N_b. The Brownian motion takes place due to the presence of nanoparticles and for the increase in N_b the Brownian motion is affected and consequently the heat transfer characteristics of the fluid changes. Increase in N_t causes increment in the thermophoresis force which tends to move nanoparticles from hot to cold side and consequently increases the temperature of the fluid.

Table 3 represents the variations in local skin friction coefficient $-f''(0)$, local Nusselt number $-\theta'(0)$ and local sherwood number $-\phi'(0)$ for various values of M, S, A^* and B^*. For stronger magnetic field the values of $-f''(0)$ and $-\phi'(0)$ increases. A very minor increase in $-\theta'(0)$ is observed with the increase in M. Negative values of $-\phi'(0)$ indicate that nanoparticle is transferred from the fluid to moving surface as discussed before. $-f''(0), -\theta'(0)$ and

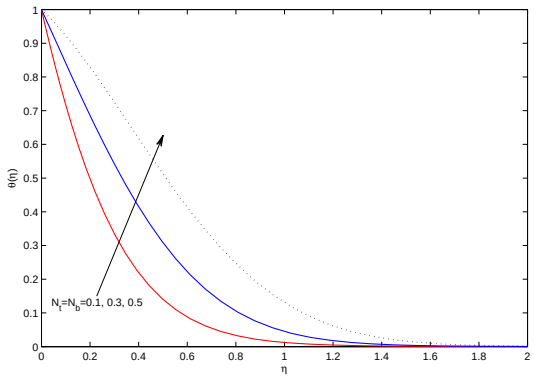

(a)

Figure 6: Effect of N_t and N_b on temperature profiles with $Pr = 6.7850,\ Le = 2,\ S = 0.5,\ A^* = 0.2,\ B^* = 0.3$, and $M = 3$

Table 3: variations of skin friction, Nusselt number and Sherwood number for various values of M, S, A^*, B^* with $Pr = 6.7850, Le = 2, N_t = 0.3$ and $N_b = 0.2$

M	S	A^*	B^*	$-f''(0)$	$-\theta'(0)$	$-\phi'(0)$
1	0.5	0.2	0.2	1.686141	2.000978	-0.955299
3				2.265564	2.037771	-1.173981
5				2.712214	2.056024	-1.305090
7				3.089454	2.065771	-1.394071
3	0.3	0.2	0.2	2.155617	1.427646	-0.600293
	0.5			2.265564	2.037771	-1.173981
	0.7			2.380394	2.686705	-1.805905
	0.9			2.500000	3.361406	-2.473698
3	0.5	-0.6	0.2	-	2.249771	-1.476083
		-0.2		-	2.144097	-1.325506
		0.2		-	2.037771	-1.173981
		0.6		-	1.930788	-1.021497
3	0.5	0.2	-0.6	-	2.218963	-1.434683
			-0.2	-	2.130147	-1.306829
			0.2	-	2.037771	-1.173981
			0.6	-	1.941409	-1.035540

$-\phi'(0)$ are the increasing function of suction parameter S. $-\theta'(0)$ and $-\phi'(0)$ are decreasing functions of heat source that is, $A^* > 0$ and $B^* > 0$ while increasing with heat sink $A^* < 0$ and $B^* < 0$.

Table 4: variations of Nusselt number and Sherwood number for various values of L_e, N_t, N_b with $Pr = 6.7850, M = 3, S = 0.5, A^* = 0.2$ and $B^* = 0.3$

Le	N_t	N_b	$-\theta'(0)$	$-\phi'(0)$
1	0.3	0.2	2.723933	-3.002687
1.5			2.309029	-1.962483
2			2.014073	-1.139920
2.5			1.796686	-0.457844
2	0.05	0.2	2.709139	0.904751
	0.1		2.553545	0.372000
	0.3		2.014073	-1.139920
	0.5		1.595297	-1.928164
	0.7		1.276229	-2.275771
2	0.3	0.1	2.523860	-5.265578
		0.2	2.014073	-1.139920
		0.3	1.572160	0.167136
		0.4	1.197889	0.769972
		0.5	0.888746	1.092839

The numerical values of $-\theta'(0)$ and $-\phi'(0)$ for different values of Le, N_t and N_b are displayed in Table 4. It is evident from table 4 that Le has decreasing influence on both $-\theta'(0)$ and $-\phi'(0)$. $-\theta'(0)$ decreases with thermophoresis and Brownian motion. As thermophoresis increases, $-\phi'(0)$ decreases, attains a minimum value and again increases in the direction from fluid to the wall. Brownian motion decreases $-\phi'(0)$, approaches a minimum value and again increases in opposite direction, that is, from the wall to the fluid.

5. Conclusions

The steady laminar, hydromagnetic nano fluid flow, heat and mass transfer adjacent to a permeable, continuously stretching sheet with linear surface velocity in the presence of magnetic, heat generation/ absorption which is a function of both space and temperature is investigated. The nonlinear governing equations for the flow are solved numerically using spectral relaxation method. Numerical results for the velocity, temperature and concentration are presented graphically for various values of parameters. In addition, Numerical data for the local skin-friction coefficient, the local Nusselt number and the local Sherwood number are tabulated for various values of magnetic field parameter, coefficients of space-dependent and time-dependent internal heat generation/absorption, suction, Lewis number, thermophoresis and the Brownian motion parameters. It is found that: The momentum boundary layer become thinner and the thermal boundary layer thickness and nanoparticle volume fraction boundary layer thickness become thicker for stronger magnetic field. The local Nusselt number and local Sherwood number decreases as both space-dependent and temperature-dependent internal heat generation coefficients increase. The opposite impact is observed as both space-dependent and temperature-dependent internal heat absorption coefficients increase. Wall fluid suction have increasing influence on the local skin friction coefficient, local Nusselt number and local sherwood number.

References

[1] W. J. Minkowycz, E. M. Sparrow, J. P. Abraham, Nanoparticle Heat Transfer and Fluid Flow, CRC Press, 2012.

[2] S. Kakac, A. Pramuanjaroenkij, Review of convective heat transfer enhancement with nanofluids, Int. J. Heat Mass Transf. 52 (2009) 3187–3196.

[3] S. U. S. Choi, Enhancing thermal conductivity of fluids with nanoparticles, in: The Proceedings of the 1995 ASME International Mechanical Engineering Congress and Exposition, San Francisco, USA, ASME, FED 231/MD 66, 1995, pp. 99-105, 1995.

[4] S. U. S. Choi, Z. G. Zhang, W. Yu, F. E. Lockwood, E. A. Grulke, Anomalously thermal conductivity enhancement in nanotube suspensions, Appl. Phys. Lett. 79 (2001) 2252–2254.

[5] C. Kleinstreuer, J. Li, J. Koo, Microfluidics of nano-drug delivery, Int. J. Heat Mass Transf 51 (2008) 5590–5597.

[6] L. Capretto, W. Cheng, M. Hill, X. Zhang, Micromixing within microfluidic devices, Top Curr Chem 304 (2011) 27–68.

[7] M. J. Uddin, W. A. Khan, A. I. Ismail, MHD free convective boundary layer flow of a nanofluid past a flat vertical plate with newtonian heating boundary condition, PLoS ONE 7(11) (2012) e49499.

[8] L. J. Crane, Flow past a stretching plate, Z. Angrew. Math. Phys. 21 (1970) 645–647.

[9] W. A. Khan, I. Pop, Boundary layer flow of nanofluid past a stretching sheet, Int. J. Heat Mass Transf 53 (2010) 2477–2483.

[10] M. Hassani, M. M. Tabar, H. Nemati, G. Domairry, F. Noori, An analytical solution for boundary layer flow of a nanofluid past a stretching sheet, Int. J. Thermal Sci. 50(11) (2011) 2256–2263.

[11] O. D. Makinde, A. Aziz, Boundary layer flow of a nanofluid past a stretching sheet with a convective boundary condition, Int. J. Thermal Sci. 50 (2011) 1326–1332.

[12] M. A. A. Hamad, M. Ferdows, Similarity solutions to viscous flow and heat transfer of nanofluid over nonlinearly stretching sheet, Appl. Math. Mech. 33(7) (2012) 923–930.

[13] F. G. Awad, P. Sibanda, A. A. Khidir, Thermodiffusion effects on magneto nanofluid flow over a stretching sheet, Boundary Value Problems 2013:136.

[14] M. Salari, M. M. Tabar, A. M. Tabar, Numerical solutions to heat transfer of nanofluid flow over stretching sheet subjected to variations of nanoparticle volume fraction and wall temperature, Appl. Math. Mech. 35 (2014) 63–72.

[15] W. Ibrahim, B. Shankar, MHD boundary layer flow and heat transfer of a nanofluid past a permeable stretching sheet with velocity, thermal and solutal slip boundary conditions, Computers and fluids 75 (2013) 1–10.

[16] W. Ibrahim, B. Shankar, M. M. Nandeppanavar, MHD stagnation poiont flow and heat transfer due to nanofluid towards a stretching sheet, Int. J. Heat Mass Transf. 56 (2013) 1–9.

[17] O. D. Makinde, W. A. Khan, Z. H. Khan, Buoyancy effects on MHD stagnation point flow and heat transfer of a nanofluid past a convectively heated stretching/shrinking sheet, Int. J. Heat Mass Transf 62 (2013) 526–533.

[18] M. Qasim, Z. H. Khan, W. A. Khan, I. A. Shah, MHD boundary layer slip flow and heat transfer of ferrofluid along a stretching cylinder with prescribed heat flux, PLoS ONE 9(1) (2014) e83930.

[19] K. Bhattacharyya, G. Layek, Magnetohydrodynamic boundary layer flow of nanofluid over an exponentially stretching permeable sheet, Physics Research International 2014 (2014) 592536.

[20] J. C. Crepeau, R. Clarksean, Similarity solutions of natural convection with internal heat generation, J. Heat Transf. 119(1) (1997) 183–185.

[21] A. Postelnicu, T. Grosan, I. Pop, Free convection boundary layer over a vertical permeable flat plate in a porous medium with internal heat generation, Int. Comm. Heat Mass Transfer 27 (2000) 729–738.

[22] E. M. Abo-Eldahab, M. A. El-Aziz, Blowing/suction effect on hydromagnetic heat transfer by mixed convection from an inclined continuously stretching surface with internal heat generation/absorption, Int. J. Thermal Sci. 43 (2004) 709–719.

[23] M. S. Abel, P. G. Siddheshwar, M. M. Nandeppanavar, Heat transfer in a viscoelastic boundary layer flow over a stretching sheet with viscous dissipation and nonuniform heat source, Int. J. Heat Mass Transf 50 (2007) 960 – 966.

[24] R. Bataller, Viscoelastic fluid flow and heat transfer over a stretching sheet under the effects of a non-uniform heat source, viscous dissipation and thermal radiation, Int. J Heat Mass Transf 50 (2007) 3152–3162.

[25] R. Tsai, K. Huang, J. Huang, Flow and heat transfer over an unsteady stretching surface with non-uniform heat source, Int. Comm. Heat Mass Transfer 35 (2008) 1340–1343.

[26] M. S. Abel, M. N. Mahantesh, Heat transfer in MHD viscoelastic boundary layer flow over a stretching sheet with non uniform heat source/sink, Comm. Nonliear. Sci. Numer. Simulat. 14 (2009) 2120–2131.

[27] G. K. Ramesh, B. J. Gireesha, C. S. Bagewadi, MHD flow of a dusty fluid near the stagnation point over a permeable stretching sheet with non-uniform source/sink, Int. J. Heat Mass Transfer 55 (2012) 4900–4907.

[28] L. Zheng, N. Liu, X. Zhang, Maxwell fluids unsteady mixed flow and radiation heat transfer over a stretching permeable plate with boundary slip and nonuniform heat source/sink, J. Heat Transf. 135 (2013) 031705–1.

[29] S. S. Motsa, A new spectral relaxation method for similarity variable non linear boundary layer flow systems, Chem. Eng. Comm. 201 (2014) 241–256.